VOL. 7, NO. 1, JANUARY 2012 ISSN 1819-6608
ARPN Journal of Engineering and Applied Sciences


www.arpnjournals.com

DISTINGUISHING LAND USE TYPES USING SURFACE ALBEDO AND NORMALIZED DIFFERENCE VEGETATION INDEX DERIVED FROM THE SEBAL MODEL FOR THE ATANKWIDI AND AFRAM SUB-CATCHMENTS IN GHANA

Tayari Salifu[1] and Wilson Agyei Agyare[2]
[1]Department of Agricultural Engineering, Bolgatanga Polytechnic, Bolgatanga, Ghana
[2]Department of Agricultural Engineering, Kwame Nkrumah University of Science and Technology, Kumasi, Ghana
E-Mail: sahakpema@yahoo.com

ABSTRACT

Distinguishing land use types is mostly done through field surveys which does not easily capture the spatial changes in the land use/cover types. In this study, the Surface Energy Balance Algorithm for Land (SEBAL) model was used to estimate surface albedo and NDVI, for different land use/cover types for two sub-catchments (i.e., Atankwidi and Afram) in the Volta Basin of Ghana. The mean coefficient of variation (CV) for individual land use/cover types compared to the mean CV for a given site was then used to distinguish among the land use/cover types. It was found that these parameters derived from the SEBAL model can be used to distinguish among different land use/cover types in the two sub-catchments. SEBAL estimates for surface albedo and NDVI across the different land use/cover types varied from 0.05 to 0.22 and -0.41 to 0.38, respectively. The range of CVs for surface albedo and NDVI, were 5-22% and 7-175%, respectively across the different land use/cover types for the two catchments. The results of this study demonstrate that SEBAL's derived surface albedo and NDVI can be used to distinguish land use/cover types in catchments similar to those of the study areas with few ground measurements.

Keywords: land use, surface albedo, NDVI, SEBAL, landsat, Ghana.

INTRODUCTION

Land use and land cover change is a key component of global change (Dale *et al*., 2000; Vitousek *et al*., 1997). Its mapping is becoming increasingly important as many countries are continuously planning to overcome the problems of indiscriminate and uncontrolled development that deteriorates the environment, leads to loss of productive agricultural lands, destruction of important wetlands, and loss of biodiversity. Land use maps and data are needed in the analysis of environmental processes and problems that must be understood if living conditions and standards are to be improved or maintained at current levels. This study is to identify appropriate methodology that can enhance the ease of distinguishing among land use type and therefore can be used in the future for mapping out land use/cover changes. To accomplish this, surface albedo and NDVI being two key characteristics of land cover were used.

Surface albedo is the ratio of the reflected radiation to the incident shortwave radiation. It is a key terrestrial variable, which is important for calculation of the Earth surface energy and water balance. Knowledge of the temporal and spatial dynamics of surface albedo is key information in investigating the earth's climate and its variability at multiple time scales (Allen *et al*., 2007a). Its distribution is therefore important for planning of irrigation schedule and estimation of water resources in agricultural areas (Tani, 1997).

NDVI is the ratio of the differences in reflectivity for the near-infrared band and the red band to their sum. It is a sensitive indicator of the amount and condition of green vegetation and it is mostly used for monitoring characteristics and changes in vegetation (Allen *et al*., 2007b). It is also used for accurate assessment of vegetation phenology, estimation of Net Primary Production (NPP) as well as the interpretation of the impact of climatic events on the biosphere (Potter and Brooks, 1998). Surface albedo can be used to distinguish NDVI for tall and short vegetation types that have similar chlorophyll content and canopy density and therefore similar NDVI, but different albedo (surface albedo is lower for taller vegetation due to shading) (Allen *et al*., 2007a).

Most commonly used methods such as using albedometers (Oguntunde, 2004), photographs (Gold and Asher, 1976), pyranometers (Platt and Griffiths, 1964) and NDVI meters (Keiffer, 2009) for estimating surface albedo and NDVI only provide estimates for a specific location (i.e., point data). This is usually not suitable for climate studies and spatial modelling. Data collection for computations of these parameters is sometimes difficult due to inaccessibility of the area in question. During the last two to three decades, significant progress has been made to estimate these parameters using satellite remote sensing (Engman and Gurney, 1992; Kustas and Norman, 1996; Bastiaanssen *et al*., 1998; Bastiaanssen *et al*., 2002; Kustas *et al*., 2003). In the past, there have been several empirical and theoretical models available to calculate surface albedo (Platt and Griffiths, 1964; Winkler and Anderson, 1954; Sellers, 1965; Wright, 1982).

The SEBAL model is a remote sensing algorithm used to compute the surface energy balance on an instantaneous time scale and for each pixel of a satellite image (Bastiaanssen, 2000; Bastiaanssen *et al*.,

1998). It has been used for many studies including water balance estimations (Pelgrum and Bastiaanssen, 1996); irrigation performance assessment studies (Roerink, 1997) and for weather prediction studies (Van de Hurk, 1997). The model has been applied in different basins of the world, e.g., Snake River Basin in Idaho, USA (Allen *et al*., 2002), the Lake Naivasha drainage basin in Kenya (Farah, 2001), all River Basins in Sri Lanka (Bastiaanssen and Chandrapala, 2003) and the Indus Basin in Pakistan (Bastiaanssen, 2002). In Ghana, Compaoré (2006) successfully used the SEBAL model to compute actual evapotranspiration in part of the Volta Basin, in the Upper East Region of Ghana. In addition, Compaoré *et al.*, (2007) used the SEBAL model to map evapotranspiration in the White Volta Basin of Ghana, West Africa using Landsat and MODIS images.

In this study, the SEBAL model was used to estimate surface albedo and NDVI for seven different land use/cover types in two selected sub-catchments (i.e., Atankwidi and Afram catchments) of the Volta Basin in Ghana. The estimated parameters were then used to distinguish among these different land use/cover types.

Computation of surface albedo and NDVI

Surface albedo is defined as the ratio of the reflected radiation to the incident shortwave radiation. It is computed using equation (1).

$$\alpha = \frac{\alpha_{toa} - \alpha_{path\_radiance}}{\tau_{sw}^2} \quad (1)$$

Where, $\alpha_{path\_radiance}$ is the average fraction of the incoming solar radiation across all bands that is back-scattered to the satellite before it reaches the earth's surface, and τ_{sw} is the atmospheric transmissivity. Values for $\alpha_{path\_radiance}$ range between 0.025 and 0.04 and for SEBAL a value of 0.03 was recommended by Bastiaanssen *et al.,* (1998).

Atmospheric transmissivity (τ_{sw}) is defined as the fraction of incident radiation that is transmitted by the atmosphere and it represents the effects of absorption and reflection occurring within the atmosphere. It includes transmissivity of both direct solar beam radiation and diffuse (scattered) radiation to the surface and is calculated assuming clear sky and relatively dry conditions using an elevation-based relationship from equation (2) (Compaoré, 2006).

$$\tau_{sw} = 0.75 + 2 \cdot 10^{-5} \cdot z \quad (2)$$

Where, z is the elevation above sea level (m).

The albedo at the top of the atmosphere (α_{toa}) is computed using equation (3).

$$\alpha_{toa} = \Sigma (\omega_\lambda \times \rho_\lambda) \quad (3)$$

Where, ρ_λ is the reflectivity and ω_λ is a weighting factor for each band.

The weighting factor for each band is computed by equation (4).

$$w_\lambda = \frac{ESUN_\lambda}{\sum ESUN_\lambda} \quad (4)$$

The reflectivity of a surface is defined as the ratio of the reflected radiation flux to the incident radiation flux. The reflectivity for each band (ρ_λ) is computed using equation (5) for Landsat images.

$$\rho_\lambda = \frac{\pi \cdot L_\lambda}{ESUN_\lambda \cdot \cos\theta \cdot d_r} \quad (5)$$

Where, L_λ is the spectral radiance for each band, $ESUN_\lambda$ is the mean solar exo-atmospheric irradiance for each band in W m^{-2} μm^{-1}, cos θ is the cosine of the solar incidence angle (from nadir), and d_r is the inverse squared relative earth-sun distance.

d_r is computed using equation (6) (Compaoré, 2006).

$$d_r = 1 + 0.033 \cos\left(DOY \frac{2\pi}{365}\right) \quad (6)$$

Where, DOY is the sequential day of the year and the angle (DOY × 2π/365) is in radians. Values for d_r range from 0.97 to 1.03 and are dimensionless.

The spectral radiance for each band (L_λ) is the outgoing radiation energy of the band observed at the top of the atmosphere by the satellite. It is calculated using equation (7) for Landsat 5 and 7.

$$L_\lambda = \left(\frac{L_{MAX} - L_{MIN}}{QCALMAX - QCALMIN}\right)(DN - QCALMIN) + L_{MIN} \quad (7)$$

Where, L_λ is the spectral radiance for each band in W m^{-2} sr^{-1} μm^{-1}, DN is the digital number of each pixel, LMIN and LMAX are calibration constants, QCALMIN and QCALMAX are the highest and lowest range of values for rescaled radiance in DN.

For Landsat 5, QCALMAX = 255 and QCALMIN = 0 so equation (7) becomes:

$$L_\lambda = \left(\frac{L_{MAX} - L_{MIN}}{255}\right) DN + L_{MIN} \quad (8)$$

Landsat 7 ETM + images provide calibration constants in the header files of each satellite image. The spectral radiance (L_λ) for each band is calculated using equation (9) (NASA, 2002):

$$L_\lambda = gain(DN) + offset \quad (9)$$

Where, gain and offset values are given in the header file of the landsat image.

Computation of normalized difference vegetation index (NDVI)

The NDVI is the ratio of the differences in reflectivity for the near-infrared band (ρ_4) and the red band (ρ_3) to their sum. It is computed using equation (10).

$$NDVI = (\rho_4 - \rho_3) / (\rho_4 + \rho_3) \quad (10)$$

MATERIALS AND METHODS

The study area

The study was carried out in two sub-catchments in the Volta Basin of Ghana - the Ghanaian part of the Atankwidi catchment and the Afram catchment (Figure-1). The Atankwidi River is a tributary of the White Volta, flowing south from Burkina Faso into the Upper East Region of Ghana between Navrongo and Bolgatanga. The Atankwidi catchment has an area of 276 km^2 and Ghanaian part covers an area of 159 km^2. The predominant occupation is rain-fed subsistence farming with shallow ground water along stream and river channels during the dry season (Martin, 2006). It is a typical agricultural catchment. The Afram River is a tributary to the Main Volta, starting from the western part of the Ejura-Sekyedumase District in the Ashanti Region of Ghana and flowing eastwards into the Volta. The Afram catchment has an area of about 300 km^2 with agriculture being the principal occupation of the inhabitants.

The Atankwidi catchment is characterized by a mono-modal rainfall distribution with a distinct rainy season lasting approximately from May to September. The long-term mean annual rainfall in Navrongo near the study area is 990 mm. Temperatures are high throughout the year with an average daily maximum temperature of 35°C and average daily minimum temperature of 23°C. Relative humidity is highest (65%) during the rainy season. It drops quickly after the end of the rainy season in October, reaching a low value of less than 10% during the Harmattan period in December and January (Martin, 2006).

The Afram catchment is characterized by two rainy seasons (Agyare, 2004). It experiences a double maxima rainfall regime. Mean annual rainfall is about 1300 mm with a very high annual and monthly variability (Adu and Mensah-Ansah, 1995). The average temperature is 26.6 °C, with the highest mean monthly temperature in March just before the onset of the rains. Relative humidity in the Afram catchment is usually more than 90% during the night and early morning.

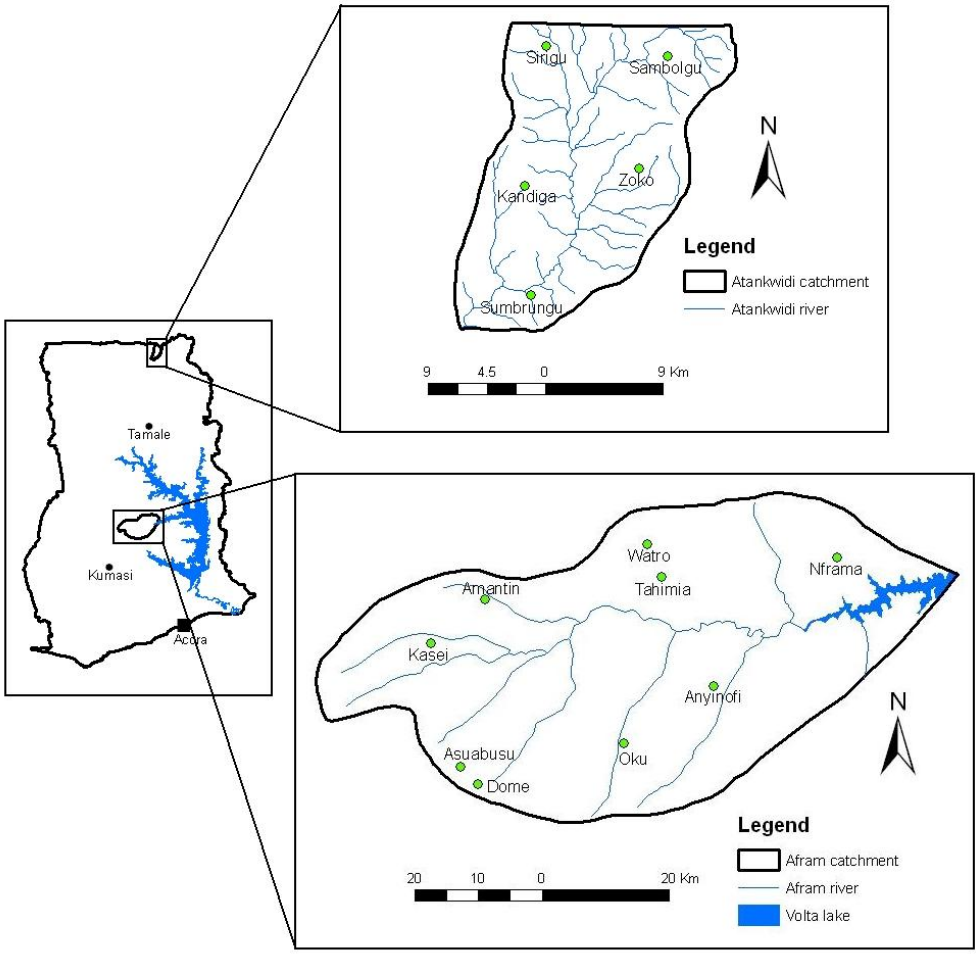

Figure-1. Location map of the study area.

The Atankwidi catchment is in the Sudan savannah. The catchment is characterized by few and scattered trees such as the baobab (Adansonia digitata), locust bean (Parkia biglobosa), acacias (Acacia spp.) and sheanut (Butyrospermum parkii). Annual burning, grazing by livestock and intensive cultivation have left the vegetation with a few trees giving rise to an open vegetation dominated by short grasses (Codjoe, 2004). The Afram catchment is of the transitional forest-savannah ecology, which lies between the Guinea savannah zone to the north and the forest vegetation to the south. The vegetation in the Afram catchment is composed of short branching trees, predominantly less than 15 meters high, which do not usually form a closed canopy and are widely scattered. The ground flora consists of apparently continuous layers of grass, some species of which reach a height of about 4 meters (Codjoe, 2004).

Soils in the Atankwidi catchment consist of lithic leptosols, fluvisols, gleyic lixisols and haplic arenosols. Lithic leptosols are predominant along the elevated northern and eastern border of the catchment. In the Afram catchment, the soils consist of dystric leptosols, ferric lixisols, haplic luvivisols and dystric fluvisols (Adu and Mensah-Ansah, 1995). Haplic luvisols are the predominant soil type.

Field data collection and parameter extraction

Six (6) satellite images - three (3) for each sub-catchment were used for the study (Table-1). These were downloaded from the University of Maryland and United States Geological Survey (USGS) websites.

Table-1. Dates of landsat images used for the study.

Catchment	Date	Path/Row
Atankwidi	November 11, 1989	194/53
	November 7, 1999	194/53
	November 7, 2005	194/53
Afram	January 1, 1986	194/54
	March 20, 2002	194/54
	January 13, 2007	194/53

Field identification of land use/cover types

In order to identify the different land use/cover types in the sub-catchments, an extensive field work was carried out from November 1, 2009 to November 13, 2009 at the Atankwidi catchment and from March 15, 2010 to March 31, 2010 at the Afram catchment. Different land use/cover types (closed woodlands, gallery forests, open woodlands, farmlands, water bodies, barelands, rocky areas and built-up areas) were mapped using a hand-held Global Positioning System (GPS) unit. All land use/cover types mapped on the field were evenly distributed over the whole catchment. Five (5) GPS points corresponding to each selected land use/cover type were taken.

Extraction of surface albedo and NDVI maps

The SEBAL Level 1 Flat Model was implemented (Compaoré *et al*., 2007) to generate the surface albedo and NDVI maps for the two sub-catchments using Erdas Imagine 9.2 as used by Salifu *et al*., (2011). The GPS coordinates for the different land use/cover types were used to extract the surface albedo and NDVI for each individual land use/cover type using ArcGIS 9.3. The mean surface albedo and NDVI is found from the five data points collected.

Data analysis

The mean, standard error (SE) and coefficient of variation (CV) for each land use/cover type were computed for all the data using Microsoft office Excel. The variability of the data in the two catchments was assessed using Equation 3.

$$CV = \left(\text{Standard}\frac{\text{Deviation}}{\text{Mean}}\right)100 \quad (11)$$

RESULTS AND DISCUSSIONS

Surface albedo distribution for atankwidi catchment

Figure-2 illustrates the surface albedo distribution for the different images (November 11, 1989; November 7, 1999 and November 7, 2005) at Atankwidi catchment. Table-2 presents the mean and standard error of surface albedo by land use/cover types at Atankwidi catchment on November 11, 1989; November 7, 1999 and November 7, 2005.

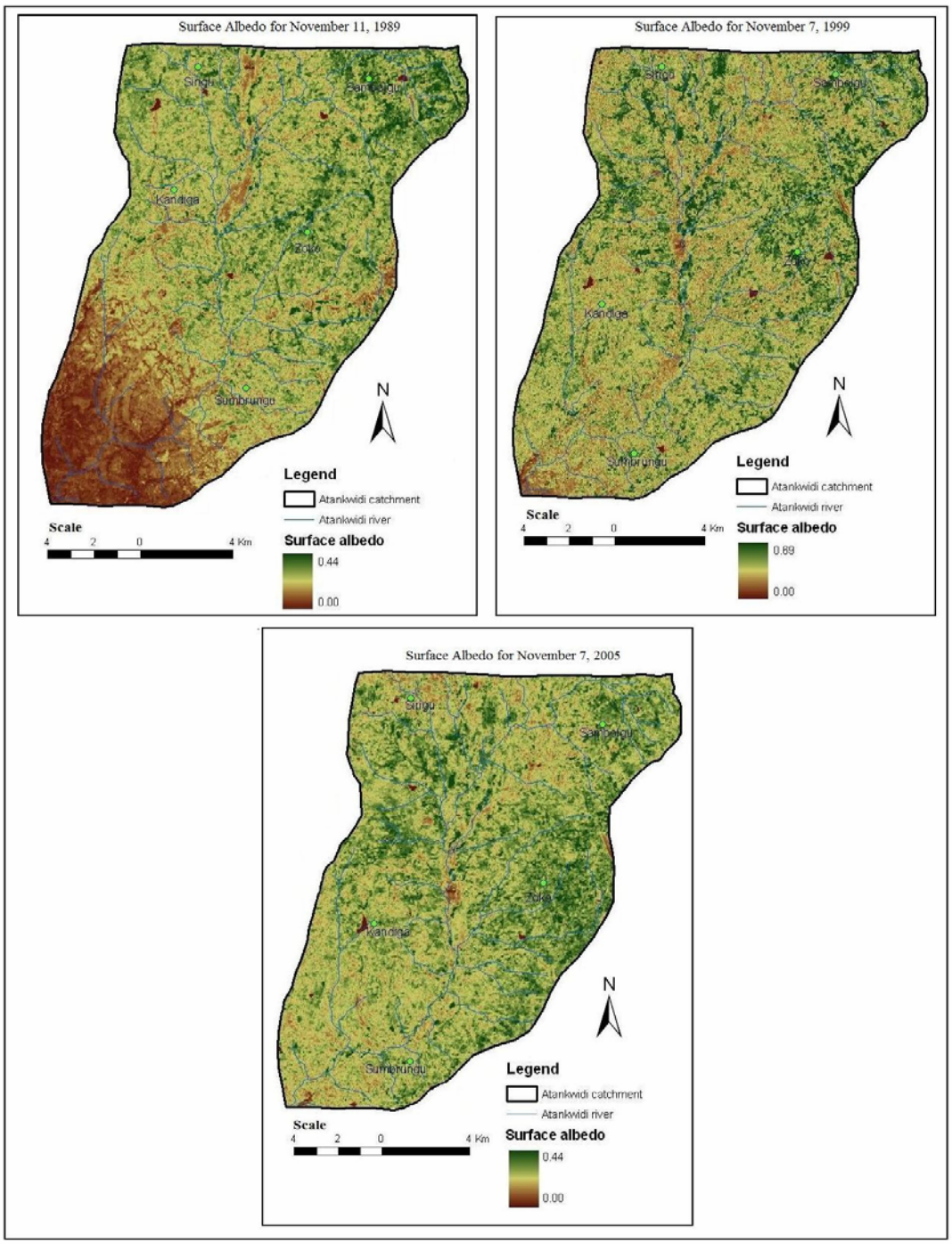

Figure-2. Surface albedo maps of Atankwidi catchment.

From the November 11, 1989 image high surface albedo values were obtained in cultivated areas and barelands and low values along rivers, water bodies and in densely vegetated areas. The range of 0.16-0.22 obtained is comparable to values presented by Compaoré (2006). The mean surface albedo over the entire land use/cover types was 0.16 with a standard error of 0.01. The mean coefficient of variation is 29% across the different land use/cover types. The CV range for the different land use/cover types is 6-20% with water bodies having the highest CV of 20% while built-up areas, open woodlands and rocky areas had the lowest CV of 6%. The high CV of 20% for water bodies compared to the value of 13.8% by Compaoré (2006) may be due to the different water bodies having different characteristics such as depth and sediment level. The CV of 11% for barelands is similar to values of

12.9% and 12.2% obtained by Oguntunde (2004) and Compaoré (2006).

Relatively high surface albedo values were found over the whole image of November 7, 1999. The exception was along rivers and water bodies which agree with the results obtained by Compaoré (2006) in the Volta Basin (Figure-2). The range of albedo values were 0.11-0.23 is similar to that reported by Compaoré (2006) and Oguntunde (2004) (0.17-0.26). The mean surface albedo across the different land use/cover types was 0.19 with 21% CV. Barelands and built-up areas had the highest and lowest CV values of 20 and 9%, respectively. The CV range of 9-20% is similar to the range presented by Compaoré (2006).

High albedo values were also observed in open woodlands and low values on densely vegetated areas, water bodies and along rivers as in Compaoré (2006) for the November 7, 2005 image. The mean surface albedo across the different land use/cover types was 0.11 with a CV of 27%.Water bodies had the highest (20%) CV with rocky areas having the lowest (8%) CV. The CV range 8-20% is similar to that presented by Compaoré (2006).

Table-2. Mean surface albedo, standard error (SE) and coefficient of variation (CV) by land use/cover types at Atankwidi catchment.

LULC Type	November 11, 1989			November 7, 1999			November 7, 2005		
	Mean	**SE**	**CV** (%)	**Mean**	**SE**	**CV** (%)	**Mean**	**SE**	**CV** (%)
Closed woodlands	0.16	0.010	13	0.18	0.01	11	0.11	0.003	9
Open woodlands	0.17	0.004	6	0.20	0.01	10	0.11	0.003	9
Farmlands	0.17	0.010	12	0.19	0.01	11	0.11	0.002	9
Water bodies	0.10	0.010	20	0.11	0.01	18	0.05	0.004	20
Barelands	0.18	0.010	11	0.20	0.01	20	0.13	0.004	15
Rocky areas	0.18	0.004	6	0.21	0.01	10	0.12	0.003	8
Built-up areas	0.18	0.002	6	0.23	0.01	9	0.16	0.010	13

In general, farmlands, barelands, rocky areas and built-up areas show relatively higher albedo. This could be related to the reflective capacity proportional to the diurnal solar radiative variation (Compaoré, 2006). In contrast, open and closed woodlands as well as water bodies show relatively low albedo values. This may be attributed to the high absorption capacity of incoming radiation due to the development of green dark algae in pond water or the green nature of vegetation.

Surface albedo distribution for Afram catchment

Illustrated on Figure-3 is the spatial distribution of surface albedo at the Afram catchment for the different images used. Also, presented on Table-3 are the mean surface albedo values for the different land use/cover types on January 11, 1986, March 20, 2002 and January 13, 2007.

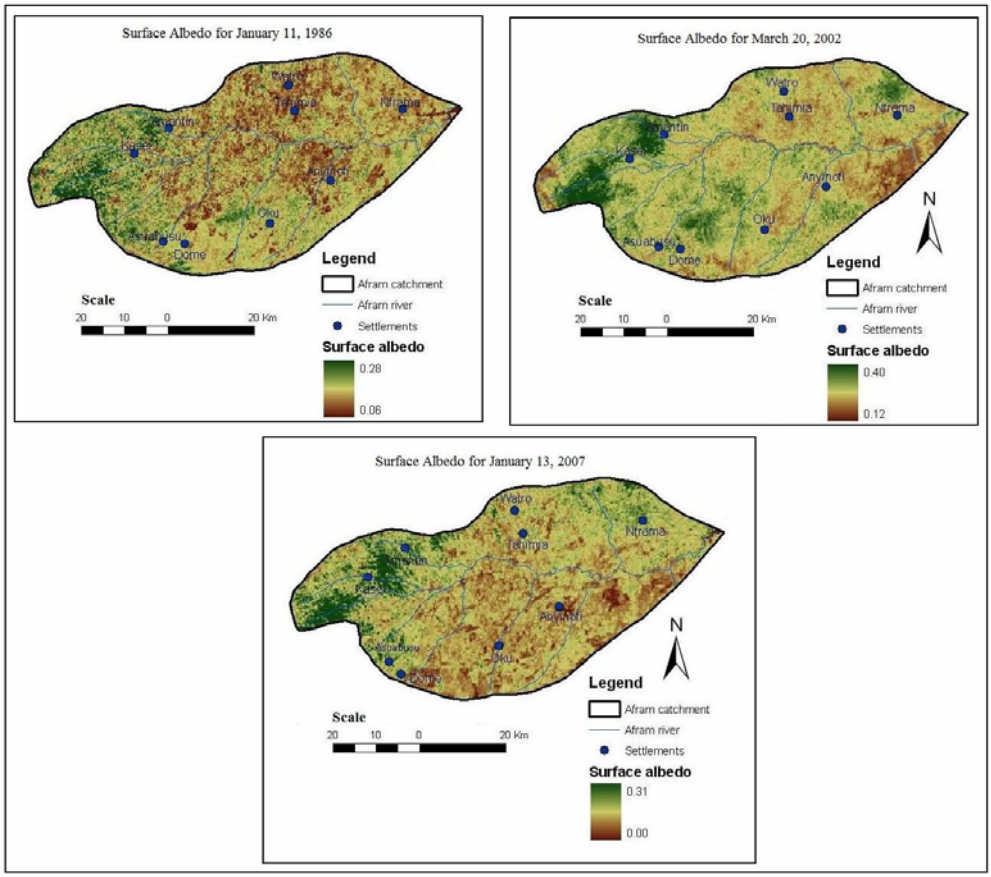

Figure-3. Surface albedo maps of Afram catchment.

High surface albedo values were found in built-up areas and low values on farmlands, closed woodlands, and water bodies for the January 11, 1986 image. The mean surface albedo across the different land use/cover types was 0.12 with a CV of 21%. The range of CV for the different land use/cover types was found to be 8-22%. Water bodies had the highest (22%) while gallery forest and closed woodlands had the lowest CV (8%).

From the March 20, 2002 image high surface albedo values were obtained in built-up areas and low values in water bodies, farmlands and closed woodlands. The mean surface albedo across the different land use/cover types was 0.20 and CV of 10%. The low CV as compared to the CVs of individual land use/cover types is due to the fact that rainfall events recorded on and a few days before the day of image acquisition. Farmlands had the highest CV of 15% while closed woodlands had the lowest CV of 5%. Water bodies and gallery forest had a CV of 6% while that of barelands and built-up areas were 10 and 9%, respectively.

Table-3. Mean surface albedo, standard error (SE) and coefficient of variation (CV) by land use/cover types at Afram catchment.

LULC Type	January 11, 1986			March 20, 2002			January 13, 2007		
	Mean	SE	CV (%)	Mean	SE	CV (%)	Mean	SE	CV (%)
Gallery Forests	0.12	0.003	8	0.18	0.003	6	0.18	0.001	6
Closed woodlands	0.11	0.003	9	0.19	0.003	5	0.16	0.002	5
Farmlands	0.12	0.003	8	0.20	0.010	15	0.18	0.005	11
Water bodies	0.09	0.005	22	0.17	0.002	6	0.15	0.002	7
Barelands	0.12	0.003	17	0.21	0.004	10	0.21	0.003	5
Built-up areas	0.13	0.005	15	0.22	0.005	9	0.20	0.004	10

Water bodies, gallery forests, farmlands and barelands had the lowest surface albedo values while higher values were observed in built-up areas in the image on January 13, 2007. The surface albedo value of 0.21 for barelands is similar to that of 0.19 for bare soil as obtained by Oguntunde (2004). The mean surface albedo across the different land use/cover types was 0.18 with a CV of 17%. Farmlands had the highest CV of 11% whiles closed woodlands and barelands had the lowest (5%). Gallery forests, built-up areas and water bodies also had CVs of 6, 10 and 7%, respectively.

The ranges of surface albedo 0.09-13, 0.18 - 0.22 and 0.15-0.21 obtained for the images of January 11, 1986; March 20, 2002 and January 13, 2007 are comparable to that presented by Compaoré (2006) (0.16-0.22) and Oguntunde (2004) (0.17-0.26).

NDVI distribution for atankwidi catchment

Figure-4 illustrates the spatial distribution of NDVI at Atankwidi catchment on November 11, 1989, November 7, 1999 and November 7, 2005. Table-4 presents the NDVI values by land use/cover types at Atankwidi catchment (11, 1989, November 7, 1999 and November 7, 2005).

Low NDVI values were found in cultivated areas, barelands and water bodies and high values along river beds and in densely vegetated areas in the November 11, 1989 image. As expected, water bodies had a negative NDVI value (between -1 and 0). The value of 0.11 for barelands is similar to the value of 0.12 for barelands as obtained by Compaoré (2006). The mean NDVI (taking the absolute value for water bodies) and CV across the land use/cover types were 0.27 and 86%, respectively. Water bodies had the highest CV of 42% with built-up areas giving the lowest CV of 7%. However, the CV of 40% for water bodies is below the value of 77.0% presented in Compaoré (2006).

For the November 7, 1999 image, relatively high NDVI values were observed along river banks and water bodies. The value of 0.10 for barelands is similar to 0.12 obtained by Compaoré (2006). The mean NDVI (taking the absolute value for water bodies) and CV across the land use/cover types were 0.31 and 81%, respectively. Barelands had the highest CV of 47% and built-up areas the lowest CV of 15%. The CVs were generally similar to those reported by Compaoré (2006) except water bodies with a value of 39% against 76.1%.

In general, closed woodlands, open woodlands and rocky areas gave high NDVI values while water bodies and barelands showed the lowest values. As expected, water bodies have a negative NDVI value. It is also observed that November, 1999 gave high NDVI values than that of November, 1986 and November, 2005. The high NDVI value found in rocky areas is due to the close proximity of the rocks to trees and grasses, thus influencing the values. The CVs range of 7-42%, 15-27% and 13-40% for November 11, 1989, November 7, 1999 and November 7, 2005 respectively are within the range of 5.4-77.0% reported by Compaoré (2006).

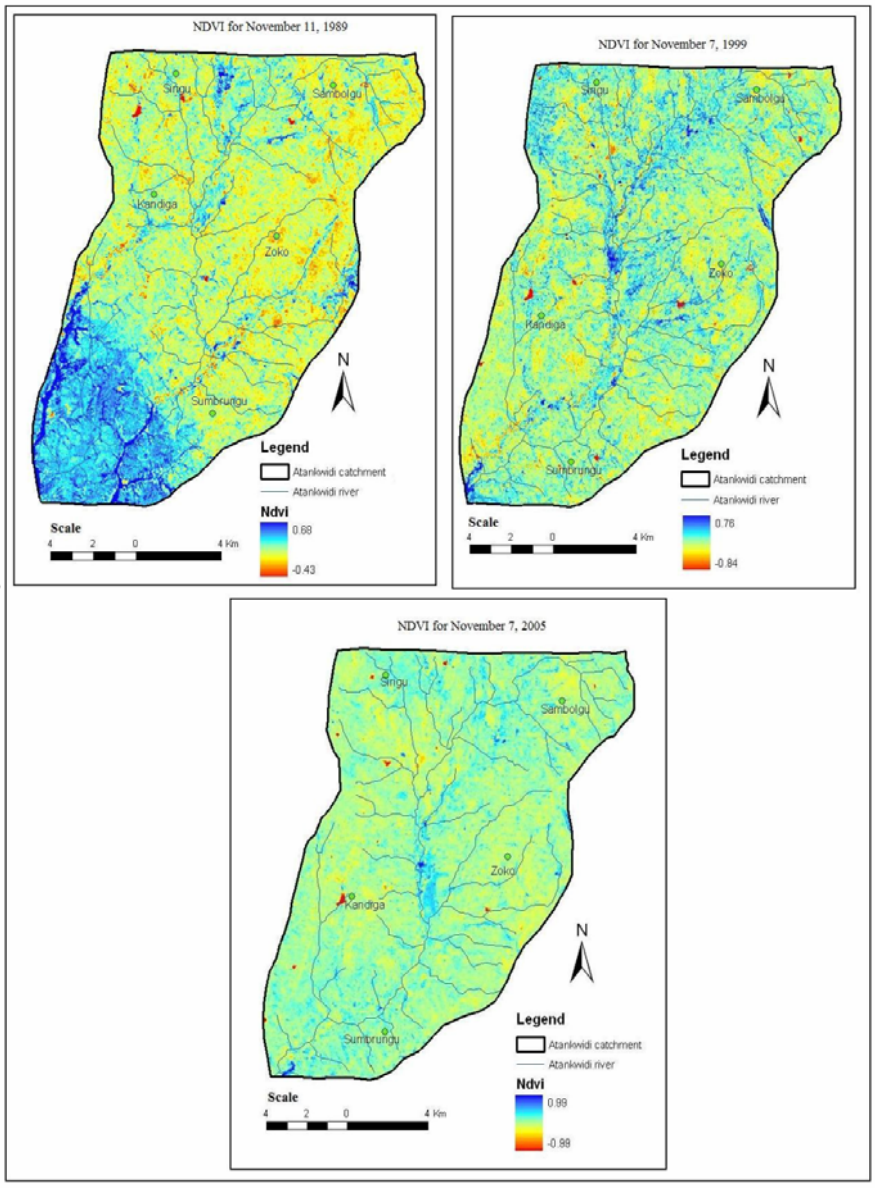

Figure-4. NDVI maps of Atankwidi catchment.

Table-4. Mean NDVI, standard error (SE) and coefficient of variation (CV) by land use/cover types at Atankwidi catchment.

LULC Type	November 11, 1989			November 7, 1999			November 7, 2005		
	Mean	SE	CV (%)	Mean	SE	CV (%)	Mean	SE	CV (%)
Closed woodlands	0.32	0.02	15	0.38	0.02	16	0.34	0.01	15
Open woodlands	0.30	0.02	23	0.33	0.02	24	0.31	0.02	19
Farmlands	0.31	0.02	19	0.41	0.02	17	0.30	0.01	13
Water bodies	-0.31	0.03	42	-0.41	0.04	39	-0.40	0.03	30
Barelands	0.11	0.02	30	0.10	0.04	47	0.11	0.02	40
Rocky areas	0.27	0.01	11	0.30	0.02	27	0.27	0.01	15
Built-up areas	0.29	0.01	7	0.27	0.01	15	0.21	0.01	19

NDVI distribution for Afram catchment

Figure-5 shows the spatial distribution of NDVI on January 11, 1986, March 20, 2002 and January 13, 2007 and Table-5 presents the NDVI values by land use/cover types for the same dates at Afram catchment.

For the image acquired on January 11, 1989, low NDVI values were obtained for water bodies and high values in gallery forests and closed woodlands. The mean NDVI (taking the absolute value for water bodies) and CV across the different land use/cover types were 0.26 and 41%, respectively Water bodies and farmlands gave the highest (27%) and lowest CV (12%), respectively. The CVs are similar to that reported by Compaoré (2006) except for water bodies.

For the March 20, 2002 image, extremely low NDVI and CV-in some cases higher than 100% were found for the different land use/cover types compared to the other images. This wide difference may be due to the rainfall events recorded on the days before image acquisition. However, the value of 0.10 for barelands is similar to 0.12 as presented by Compaoré (2006). The mean NDVI (taking the absolute value for water bodies) and CV across the different land use/cover types were 0.08 and 117%, respectively. This high variation across the various land use/cover types is because the different land use/cover types have quite significantly different NDVI values.

For the January 13, 2007 image, high NDVI values were observed for most parts of the image. Water bodies (negative), and barelands had low NDVI values whiles gallery forests, and open woodlands and farmlands were observed to have high NDVI values. The mean NDVI (taking the absolute value for water bodies) across the different land use/cover types is 0.27 with a CV 90%. Barelands have the highest CV (50%) with closed woodlands giving the value of 12%.

The ranges of CV, 12-27% and 12-50% for the images acquired on January 11, 1986 and January 13, 2007 falls within the range 5.4-77.0% as obtained by Compaoré (2006). However, the CVs were generally high (44-175%) for the March 20, 2002 image as compared to that of the other images and also to the values given by Compaoré (2006).

Generally, built-up areas, gallery forests, closed woodlands and farmlands have relatively high NDVI values greater than 1. Built-up areas gave a high NDVI value because of the vegetation (trees, vegetable gardens, and some lawns) that is mostly found in such areas. Barelands have low values and water bodies had NDVI values less than 1. January 13, 2007 image gave values that were higher than that of January 11, 1986. However, March 20, 2002 gave values much less than those two years.

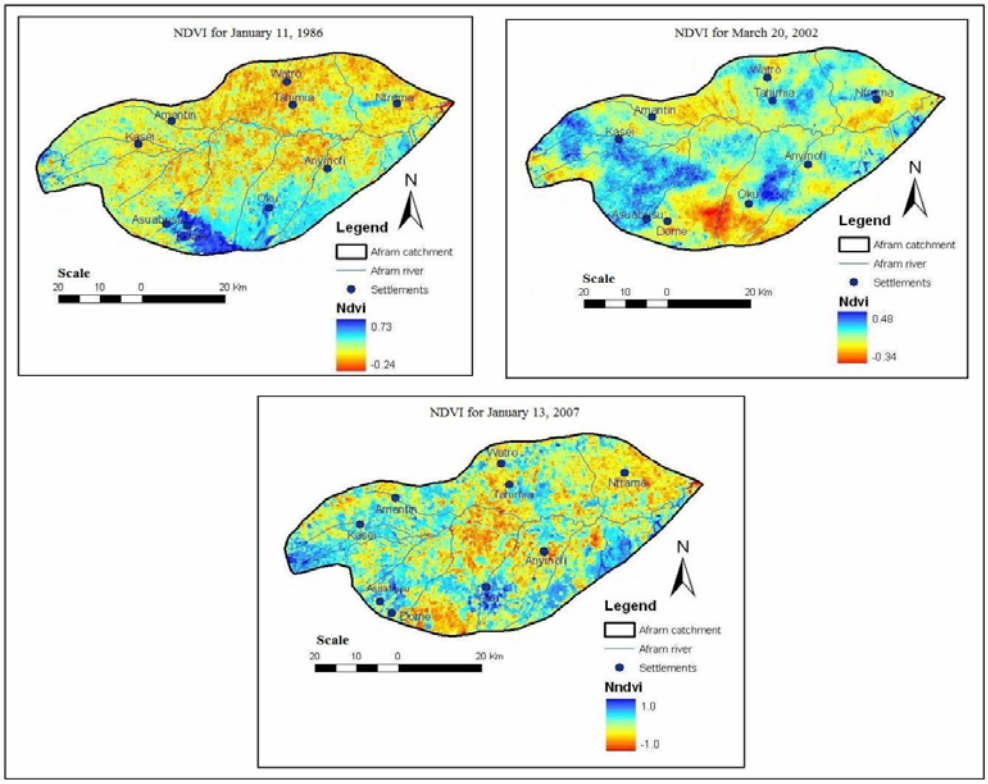

Figure-5. NDVI maps of Afram catchment.

Table-5. Mean NDVI, standard error (SE) and coefficient of variation (CV) by land use/cover types at Afram catchment.

LULC Type	January 11, 1986			March 20, 2002			January 13, 2007		
	Mean	SE	CV (%)	Mean	SE	CV (%)	Mean	SE	CV (%)
Gallery Forests	0.31	0.02	26	0.11	0.03	109	0.31	0.01	16
Closed woodlands	0.27	0.02	26	0.09	0.01	44	0.25	0.01	12
Farmlands	0.34	0.01	12	0.10	0.02	80	0.38	0.01	13
Water bodies	-0.21	0.02	27	-0.06	0.01	50	-0.22	0.02	36
Barelands	0.11	0.01	19	0.10	0.03	120	0.08	0.01	50
Built-up areas	0.30	0.01	13	0.04	0.02	175	0.35	0.01	17

CONCLUSIONS

SEBAL was successfully used to estimate surface albedo and NDVI for different land use/cover types (closed woodlands, gallery forests, open woodlands, farmlands, water bodies, barelands, rocky areas and built-up areas) in the Guinea savannah (Atankwidi) and Forest-savannah (Afram) ecologies using Landsat satellite images for the Volta Basin of Ghana.

In the two sub-catchments, mean values of surface albedo and NDVI were in the ranges of 0.05-0.23 and -0.41-0.38, respectively across the different land use/cover types. Water bodies had the lowest surface albedo and NDVI values while closed woodlands and gallery forests were observed to have the highest values. Also, the NDVI was observed to be affected greatly by rainfall, making it less suitable for distinguishing land use/cover types as compared to the surface albedo.

The range of CVs for surface albedo and NDVI were 5-22% and 7-175%, respectively across the different land use/cover types for the two catchments. The mean CVs across the different land use/cover types were higher than that of the individual land use/cover (eg. open woodlands) CVs for surface albedo and NDVI. Therefore SEBAL model distinguishes the estimated surface albedo and NDVI among the different land use/cover types in the two catchments. The only exception was on March 20, 2002 for the Afram catchment where the mean CV across the different land use/cover types for both surface albedo and NDVI were lower than the individual CVs for some land use/cover types. This may be due to the rainfall events recorded on and a few days before image acquisition.

The study has shown that the SEBAL model can be conveniently used to estimate surface albedo and NDVI and subsequently used to distinguish different land use/cover in catchments of similar characteristics such as that of the study areas.

ACKNOWLEDGEMENTS

The authors are deeply grateful to the Heads and staff of the Department of Agricultural Engineering, Bolgatanga Polytechnic, Bolgatanga and the Department of Agricultural Engineering, Kwame Nkrumah University of Science and Technology (KNUST), Kumasi for their support throughout the period of this study.

REFERENCES

Adu S.V. and Mensah-Ansah J. A. 1995. Soils of the Afram basin: Ashanti and Eastern regions, Ghana. Soil Research Institute (CSIR), Memoir No. 12: 17-53.

Agyare W. A. 2004. Soil characterization and modeling of spatial distribution of saturated hydraulic conductivity at two sites in the Volta basin of Ghana. PhD Thesis. University of Bonn, Bonn, Germany.

Allen R.G., Morse A., Tasumi M., Trezza R., Bastiaanssen W. G. M., Wright J. L. and Kramber W. 2002. Evapotranspiration from a satellite-based surface energy balance for the Snake Plain Aquifer in Idaho. Proceedings of the National USCID Conference, San LUIS Obispo, California, USA. July 8-10. pp. 161-175.

Allen R. G., Pereira L. S., Raes D. and Smith M. 1998. Crop Evapotranspiration. Guidelines for computing crop water requirements. FAO Irrigation and Drainage Paper 56, Food and Agricultural Organization of the United Nations, Rome, Italy.

Allen R. G., Tasumi M. and Trezza R. 2007a. METRICT: Mapping Evapotranspiration at High Resolution. Applications Manual for Landsat Satellite Imagery. Version 2.0.3, University of Idaho, Kimberly, Idaho, USA.

Allen R. G., Tasumi M., Morse A., Trezza R., Kramber W. and Lorite I. 2007b. Satellite-based energy balance for mapping evapotranspiration with internalized calibration (METRIC) – Applications. Journal of Irrigation and Drainage Engineering. 133: 395-406.

Bastiaanssen W. G. M. 2000. SEBAL-based sensible and latent heat fluxes in the irrigated Gediz Basin, Turkey. Journal of Hydrology. 229(1-2): 87-100.

Bastiaanssen W. G. M., Ahmad M. D. and Chemin Y. 2002. Satellite surveillance of evaporative depletion across

the Indus Basin. Water Resources Research. 38(12): 1273-1282.

Bastiaanssen W. G. M. and Chandrapala L. 2003. Water balance variability across Sri Lanka for assessing agricultural and environmental water use. Agricultural Water Management. 58(2): 171-192.

Bastiaanssen W. G. M., Menenti M., Feddes R. A. and Holtslag A. A. M. 1998. A remote sensing surface energy balance algorithm for land (SEBAL): 1. Formulation. Journal of Hydrology. 212/213: 198-212.

Codjoe S. N. A. 2004. Population and Land Use/Cover dynamics in the Volta River Basin of Ghana, 1960-2010. PhD Thesis. University of Bonn, Bonn, Germany.

Compaoré H. 2006. The impact of savannah vegetation on the spatial and temporal variation of the actual evapotranspiration in the Volta Basin, Navrongo, Upper East Ghana. PhD Thesis. University of Bonn, Bonn, Germany.

Compaoré H., Hendrickx J. M. H., Hong S., Friesen J., van de Giesen N. C., Rodgers C., Szarzynski J. and Vlek P. L. G. 2007. Evaporation mapping at two scales using optical imagery in the White Volta Basin, Upper East Ghana. Physics and Chemistry of the Earth. [DOI: 10.101 6/j .pce.2007.04.021].

Dale V.H., Brown S., Haeuber R.A., Hobbs N.T., Huntly N., Naiman J., Riebsame W. E, Turner M. G. and Valone T. J. 2000. Ecological principles and guidelines for managing the use of land. Ecol. Appl. 3: 639-670.

Engman E. T. and Gurney R. J. 1992. Remote sensing in hydrology. Chapman and Hall, London, U.K.

Farah H. O. 2001. Estimation of regional evaporation under different weather conditions from satellite and meteorological data: A case study of the Navaisha Basin. PhD Thesis. ITC, Wageningen, Netherlands.

Gold A. and Asher J. B. 1976. Soil reflectance using a photographic method. Soil Science Society. 40(3): 337-341.

Keiffer D. L. 2009. NDVI meter: product manual. Spectrum Technologies Inc., Illinois.

Kustas W. P. and Norman J. M. 1996. Use of remote sensing for evapotranspiration monitoring over land surfaces. Hydrological Science Journal. 4(4): 495-515.

Kustas W. P., Diak G. R. and Moran M. S. 2003. Evapotranspiration and Remote Sensing: Encyclopedia of Water Science Marcel Dekker, Inc., New York.

Martin N. 2006. Development of a water balance for the Atankwidi catchment, West Africa-A case study of groundwater recharge in a semi-arid climate. PhD thesis, University of Bonn, Bonn, Germany.

Oguntunde P. G. 2004. Evapotranspiration and complimentarity relations in the water balance of the Volta Basin: Field measurements and GIS-based regional estimates. PhD Thesis. University of Bonn, Germany.

Pelgrum H. and Bastiaanssen W. G. M. 1996. An inter-comparison of techniques to determine the area-averaged latent heat flux from individual in situ observations: A remote sensing approach using the European Field Experiment in a desertification-threatened area data. Water Resources Bulletin. 32: 2775-2786.

Platt R. B. and Griffiths J. 1964. Environmental measurement and interpretation. Reinhold Publishing Corporation, New York, USA.

Potter C. S. and Brooks V. 1998. Global analysis of empirical relations between annual climate and seasonality of NDVI. International Journal of Remote Sensing. 19(15): 2921-2948.

Roerink G. J. 1997. Relating crop water consumption to irrigation water supply by remote sensing. Water Resources Management. 11: 445-465.

Salifu T., Agyare W. A., Kyei-Baffour N., Mensah E. and Ofori E. 2011. Estimating actual evapotranspiration using the SEBAL model for the Atankwidi and Afram catchments in Ghana. International Journal of Applied Agricultural Research. 6(2): 177-193.

Sellers W. D. 1965. Physical Climatology. The University of Chicago University Press, Chicago, USA.

Tani H. 1992. Estimation of surface albedo from NOAAAVHRR data. Journal of the Faculty of Agriculture, Hokkaido University. 65(4): 331-341.

Van de Hurk B. J. J. M., Bastiaanssen W. G. M., Pelgrum H. and van Meijgaard E. 1997. A new methodology for assimilation of initial soil moisture fields in weather prediction models using Meteosat and NOAA data. Journal of Applied Meteorology. 36: 1271-1283.

Vitousek P. M., Money H. A., Lubchenco J. and Melillo J. M. 1997. Human domination of Earth's ecosystems. Science. 277: 494-499.

Winkler J. R. and Anderson K. 1954. Geomagnetic and albedo studies with a Cerenkov Detector at 40 degree geomagnetic latitude. Physical Review. 93(3): 596-605.

Wright J. L. 1982. New evapotranspiration crop coefficients. Journal of Irrigation and Drainage Division, ASCE. 108(2): 57-73.